Dynamics of Localized Modes in a Composite Multiferroic Chain

L. Chotorlishvili,[1] R. Khomeriki,[2,3] A. Sukhov,[1] S. Ruffo,[4] and J. Berakdar[1]

[1]*Institut für Physik, Martin-Luther-Universität Halle-Wittenberg, D-06120 Halle/Saale, Germany*
[2]*Physics Department, Tbilisi State University, 0128 Tbilisi, Georgia*
[3]*Max Planck Institute for the Physics of Complex Systems, Nöthnitzer Strasse 38, 01187 Dresden, Germany*
[4]*Dipartimento di Fisica e Astronomia and CSDC, Università di Firenze, CNISM and INFN, via G. Sansone 1, 50019 Sesto Fiorentino, Italy*

(Received 16 January 2013; revised manuscript received 19 August 2013; published 11 September 2013)

In a coupled ferroelectric-ferromagnetic system, i.e., a composite multiferroic, the propagation of magnetic or ferroelectric excitations across the whole structure is a key issue for applications. Of special interest is the dynamics of localized magnetic or ferroelectric modes (LM) across the ferroelectric-ferromagnetic interface, particularly when the LM's carrier frequency is in the band of the ferroelectric and in the band gap of the ferromagnet. For a proper choice of the system's parameters, we find that there is a threshold amplitude above which the interface becomes transparent and an in-band ferroelectric LM penetrates the ferromagnetic array. Below that threshold, the LM is fully reflected. Slightly below this transmission threshold, the addition of noise may lead to energy transmission, provided that the noise level is neither too low nor too high, an effect that resembles stochastic resonance. These findings represent an important step towards the application of ferroelectric and/or ferromagnetic LM-based logic.

DOI: 10.1103/PhysRevLett.111.117202 PACS numbers: 85.80.Jm, 75.78.−n, 77.80.Fm

Introduction.—Multiferroics (MF) possess coupled ferroic (magnetic, electric, or elastic) ordering [1–3]. The current high interest in MF is fueled by the impressive advances in synthesizing composite ferroelectric- (FE-) ferromagnetic (FM) nano- and multilayer structures. These show a substantially larger multiferroic coupling strength [1–5] as compared to bulk matter, so-called single-phase multiferroics [1,6] such as Cr_2O_3 [7]. MFs are important for addressing fundamental questions regarding the connection between electronic correlation, symmetry, magnetism, and polarization. They also hold the promise for qualitatively new device concepts based on exploiting the magnetoelectric (ME) coupling to steer magnetism (ferroelectricity) via electric (magnetic) fields. Potential applications are wide and range from sensorics and magnetoelectric spintronics to environmentally friendly devices with ultralow heat dissipation [8–10]. Thereby, a key issue is how efficiently magnetic or ferroelectric information, i.e., an initial excitation, is transmitted in a system with a MF coupling. For instance, in a two-phase or composite MF [1,6,11] such as $BaTiO_3/CoFe_2O_4$ [12], $PbZr_{1-x}Ti_xO_3$/ferrites [13,14], $BaTiO_3$/Fe [15], $PbTiO_3$/Fe [16,17], or $BaTiO_3$/Ni the MF coupling is strongest at the FE/FM interface, whereas away from it the FE or FM order is only marginally affected. Thus, we expect that a ferroelectric signal triggered by an electric field in the FE part may or may not be converted into a magnetic signal depending on the dynamics taking place at the interface. How this transport of information depends on the properties of the system is rarely addressed and will be studied in this Letter. The outcome of such a study would not only uncover the conditions for optimal signal handling but also holds the potential for new insights into the multiferroic coupling retrieved by tracing the signal dynamics. We will focus on weakly nonlinear localized modes (LM) which are formed by a modulation of linear excitations of the ferroelectric and the ferromagnetic systems. Such nonlinear modes have in isolated FM or FE phases a series of applications in magnetic logic, microwave signal processing, and spin electronic devices. A clear advantage is that LMs of a large number of elementary excitations are very robust and have a particlelike nature [18]. In that sense, LMs are very similar to their topological counterparts (magnetic solitons) that have been considered for logic operations [19–21]. Multiferroics offer new fascinating mechanisms for LM dynamics [22]. For example, due to discreteness and/or nonlinearity of the system, it may happen that the large-amplitude excitation frequency falls within the gap of the linear oscillations spectrum, as illustrated in Fig. 1. Then, the energy of the excitation would not spread over the lattice. As well-established in studies on intrinsic LMs, e.g., [23–30], we know that, in spite of the localized energy profile, such modes may move along the whole chain. This means that excitations created in the ferroelectric part via an electric field can be transmitted to the magnetic part and move there. Moreover, as it will be shown below, the creation of these band-gap LMs can be enhanced by noise, manifesting thus some analogy with the stochastic resonance phenomenon [31,32].

Model.—For our purposes, a large ME coupling is necessary. In this respect, new fabrication methods [14] for the so-called two-phase or composite multiferroics [1,6,11], as well as the realization of ferroelectric wires [33], are

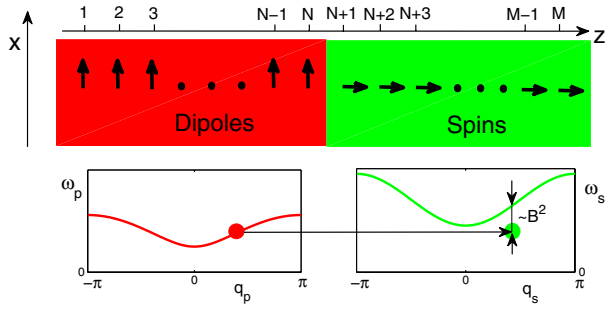

FIG. 1 (color online). Schematics of a chain consisting of a ferroelectric and a ferromagnetic part coupled at the interface. The lower panel shows a particular choice of frequency for which a conventional localized mode is formed in the ferroelectric. In the ferromagnetic part a band-gap localized excitation develops with a nonlinear frequency shift proportional to B^2 (B is the amplitude of a magnetic band-gap localized mode). The chosen mutual alignment of the ferroelectric polarization and the magnetization at the interface resembles the realized ferroelectric ($BaTiO_3$) tunnel junction with ferromagnetic (Fe) electrodes [43].

encouraging. Examples of composite multiferroics $BaTiO_3/CoFe_2O_4$ [12] or $PbZr_{1-x}Ti_xO_3$/ferrites [14] are still popular. Major research is focused on $BaTiO_3$/Fe [15], $PbTiO_3$/Fe [16,17], or $BaTiO_3$/Ni composite multiferroics, to name but a few, since their bulk parameters are very well known (Ref. [34] for $BaTiO_3$ and Ref. [35] for Fe or Ni) as well as the misfit of the lattices is relatively low [16]. Relatively high ME constants [16,17] were predicted for these materials at room temperatures. A possible mechanism for ME coupling at the FE/FM interface is based on screening effects [36]. We assume here the presence of a similar mechanism based microscopically on the rearrangement of charges and spins at the FM/FE interface, as confirmed by other studies [5,15]. The spin-polarized charge density formed in the FM in the vicinity of the FM/FE interface [36] acts with a torque on the magnetic moments in the FM, resulting in a noncollinear magnetic ordering (similar as in [37]). Hence, electric polarization emerges that couples the FM to the FE part. This picture yields a linear ME coupling with a pseudoscalar coupling constant. Technically, we describe the bulk unstrained $BaTiO_3$ by the Ginzburg-Landau-Devonshire (GLD) potential [34]. For the discretized FE polarization (P_n) in a coarse-grained approach, the form of the GLD potential for a general phase and arbitrary temperatures is quite involved [38]. However, at room temperature the $BaTiO_3$ crystal has an axis along which the polarization switches (tetragonal phase). Consequently, the form of the GLD potential reduces to the one-dimensional biquadratic potential. For the description of the magnetization (S_k) dynamics in the FM, we employ the classical Heisenberg model. S_k is discretized and normalized to the saturation value of the coarse-grained magnetization vector. With the aim of exploring the feasibility of conversion of the electric excitation formed in FE part of the sample into a localized spin magnetic excitation in FM part, we thus employ the multiferroic model (cf. Fig. 1)

$$
\begin{aligned}
&H = H_{\mathrm{P}} + H_{\mathrm{S}} + V_{\mathrm{SP}},\\
&H_{\mathrm{P}} = \sum_{n=1}^{N}\left(\frac{\alpha_0}{2}\left(\frac{dP_n}{dt}\right)^2 + \frac{\alpha_1}{2}P_n^2 + \frac{\alpha_2}{4}P_n^4 + \frac{\kappa}{2}(P_{n+1}-P_n)^2\right),\\
&H_{\mathrm{S}} = \sum_{k=N+1}^{M}(-J_1\vec{S}_k\vec{S}_{k+1} - J_2(S_k^z)^2),\\
&V_{\mathrm{SP}} = -gP_NS_1^x,
\end{aligned}
\tag{1}
$$

where H_{P} is the Hamiltonian of the FE part of the multiferroic system, describing N-interacting FE dipoles [29,38] (P_n and dP_n/dt are conjugated variables). P_n and $\vec{S}_k$ stand, respectively, for the deviations from the equilibrium positions of the nth dipole and the kth spin vector. At room temperature, we can choose the polarization vector to be directed along the x axis $\vec{P}_n = (P_n, 0, 0)$, $n = 1, \ldots, N$. α_0 is a kinetic coefficient, $\alpha_{1,2}$ are potential constants, and κ is the nearest neighbor coupling constant. H_{S} describes the ferromagnetic chain [39], where J_1 is the nearest neighbor exchange coupling in the FM part and J_2 is the uniaxial anisotropy constant. Interface effects between the spin and the FE dipole systems are described by the dipole-spin interaction Hamiltonian V_{SP}.

In our numerical simulations we operate with dimensionless quantities upon introducing $p_n = P_n/P_0$, $\vec{s}_k = \vec{S}_k/S$ and defining a dimensionless time as $t \to \omega_0 t$ ($\omega_0 = \sqrt{\kappa/\alpha_0} \sim 10^{12}$ Hz). The equations governing the time evolution of the dipoles and the spins (except for the sites near the interface) read

$$
\frac{d^2p_n}{dt^2} = -\alpha p_n - \beta p_n^3 + (p_{n-1} - 2p_n + p_{n+1}), \tag{2}
$$

$$
\frac{\partial s_k^{\pm}}{\partial t} = \pm iJ[s_k^{\pm}(s_{k-1}^z + s_{k+1}^z) - s_k^z(s_{k-1}^{\pm} + s_{k+1}^{\pm})] \pm 2iDs_k^{\pm}s_k^z, \tag{3}
$$

where $n \neq N$ and $k \neq N+1$. We have introduced the following dimensionless constants: $\alpha = \alpha_1/\kappa$, $\beta = \alpha_2P_0^2/\kappa$, $J = J_1S/\omega_0$, and $D = J_2S/\omega_0$. For the dipole p_N and the spin $\vec{s}_1$ at the interface the following equations hold:

$$
\begin{aligned}
&\frac{d^2p_N}{dt^2} = -\alpha p_N - \beta p_N^3 + (p_{N-1} - 2p_N + g_s s_1^x),\\
&\frac{\partial s_1^{\pm}}{\partial t} = \pm iJ[s_1^{\pm}s_2^z - s_1^z s_2^{\pm}] \pm i[2Ds_1^{\pm}s_1^z - g_p p_N s_1^z].
\end{aligned}
\tag{4}
$$

Here $s_k^{\pm} \equiv s_k^x \pm is_k^y$, $g_s = gS/(\kappa P_0)$, and $g_p = gP_0/(S\omega_0)$. The evolution according to Eqs. (2)–(4) proceeds under the constraint $(s_k^x)^2 + (s_k^y)^2 + (s_k^z)^2 = 1$. For the derivation of the weakly nonlinear envelope solutions from Eqs. (2) and (3) one can rely on the reductive perturbation theory

developed in Refs. [40,41]. One obtains the solutions for the dipoles and the spins separately in the following form (a detailed derivation is provided as Supplemental Material to this Letter [42]):

$$p_n = \frac{A\cos[\omega_p t - q_p n + \delta\omega_p t]}{\cosh[(n - V_p t)/\Lambda_p]}, \qquad s_k^{\pm} = \frac{Be^{\pm i(\omega_s t - q_s k + \delta\omega_s t)}}{\cosh[(k - V_s t)/\Lambda_s]}, \tag{5}$$

where A and B are the amplitudes of the dipolar and the magnetic localized excitations, respectively; ω_p and ω_s are the frequencies of the linear excitations which obey the following dispersion relations:

$$\omega_p = \sqrt{\alpha + 2(1 - \cos q_p)}, \qquad \omega_s = 2[D + J(1 - \cos q_s)], \tag{6}$$

q_p and q_s are the carrier wave numbers of the dipolar and the spin excitations; and $V_p = \sin q_p/\omega_p$ and $V_s = 2J\sin q_s$ are the group velocities of the corresponding LMs. The widths of the dipolar and spin LMs are

$$\Lambda_p = \frac{1}{A}\sqrt{\frac{2(\omega_p^4 - \alpha^2 - 4\alpha)}{3\omega_p^2\beta}}, \qquad \Lambda_s = \frac{1}{B}\sqrt{\frac{4J\cos q_s}{\omega_s}}. \tag{7}$$

The nonlinear frequency shifts are defined as

$$\delta\omega_p = A^2\frac{3\beta}{16\omega_p}, \qquad \delta\omega_s = -B^2\frac{\omega_s}{4}. \tag{8}$$

Note that, for wave packet transmission, the following matching condition between the frequencies has to be fulfilled:

$$\omega_p + \delta\omega_p = \omega_s + \delta\omega_s. \tag{9}$$

For an efficient transmission of the LM from the FE into the FM part, the widths of the LM should be the same in both parts, i.e., $\Lambda_p = \Lambda_s$ with the restriction $B \le g_p A$. If one excites the LM with a carrier frequency ω which is located within the band of both the dipolar and the spin wave spectrum, then the localization will safely penetrate from the FE to the FM part, but some portion of the energy will be reflected by the interface. By changing the amplitude of the LM, one can manipulate the ratio between the transmitted and reflected parts of the LM. In addition, the transmission is very sensitive to the coupling constant g between the FE and the FM parts. We have investigated this dependence by varying only the coupling constant g_s and fixing the values of the dimensionless parameters as follows: $\alpha = 0.2$, $\beta = 0.1$, $J = 1$, $D = 0.6$. We assume for simplicity $g_p = g_s$ (in general these constants differ, depending on the material of the samples, but this is not an obstacle for the theory).

Numerical results.—Realistic material parameters are tabulated in full detail in the Supplemental Material [42]. There, we provide explicitly the relation to the normalized units which we use below. The essential parameters entering Eq. (1) are the FE potential coefficients $\alpha_1/(a_{\mathrm{FE}}^3) = 2.77 \times 10^7$ [V m/C], $\alpha_2/(a_{\mathrm{FE}}^3) = 1.7 \times 10^8$ [V m^5/C^3], the FE coupling coefficient $\kappa/(a_{\mathrm{FE}}^3) = 1.3 \times 10^8$ [V m/C], the equilibrium polarization $P_0 = 0.265$ [C/m^2], and the coarse-grained FE cell size $a_{\mathrm{FE}} = 1$ [nm]. The FM exchange interaction strength is $J_1 = 3.15 \times 10^{-20}$ [J], the FM anisotropy constant is $J_2 = 6.75 \times 10^{-21}$ [J], and the ME coupling strength is $g \approx 10^{-21}$ [V m^2]. Figures 2(a)–2(c) show the localized energy evolution along the lattice for different values of the coupling constant g_p. In graph (d) the dependence of the transmitted energy on the coupling constant is displayed, pointing out that the transmission is maximal when g_p is in between the spin and the dipolar coupling constants (in reduced units it is equal to 1). Spin alignments, the topology of the excitation, and its propagation in the chain at different times are

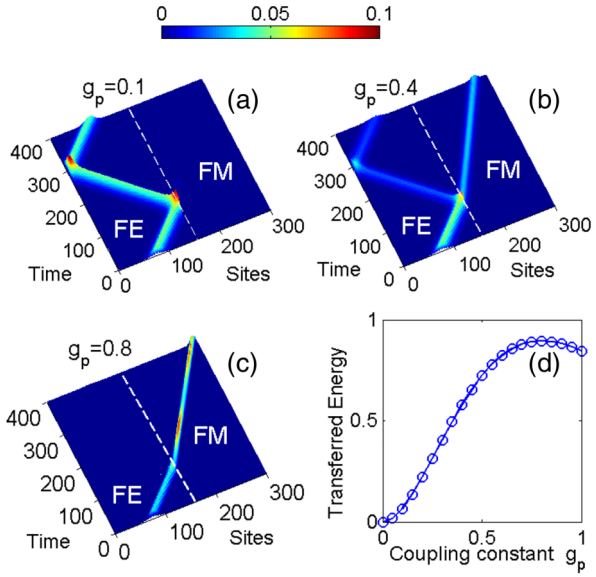

FIG. 2 (color online). Insets (a), (b), and (c) show the time and site dependence of the local energy. For dipoles this energy is given by the local values of H_{P}, and for the spins by the local values of $H_{\mathrm{S}} + S^2[J_1 + J_2]$. g_p is a coupling constant indicating the strength of the ME interface interaction. The graphs point out the LM reflection and transmission at the FE/FM interface (white dashed line). The dipolar localization carrier wave number is chosen as $q_p = 0.4\pi$ and the dipolar localization amplitude is chosen as $A = 0.2$. Dipoles and spins (separated by the white dashed line) occupy the sites $n = 1 \ldots 150$ and $k = 151 \ldots 300$, respectively. (d) Dependence of the relative energy transferred to the FM part (i.e., ratio of the energy in the FM part to the total injected energy) on the coupling constant strength g_p.

displayed in the Supplemental Material [42]. Further interesting effects arise when a band localized excitation forms with a carrier frequency ω in the band of the dipolar spectrum (see bottom panel of Fig. 1) and slightly below the zone boundary $\omega_s(q_s = 0)$ of the spin wave spectrum. Then, for small amplitudes, the dipolar LM is totally reflected by the interface because it does not resonate with any mode in the spin array. However, with increasing the amplitude, there is an $A_{\rm cr}$ value threshold (due to the nonlinear frequency shift) above which the LM is transmitted towards the FM part of the multiferroic chain, forming thus a magnetic band-gap localization. Using Eqs. (8) and (9) and assuming $B = A$, one can infer the relation defining this threshold amplitude to be

$$\omega_s(q_s = 0) - \omega = \left(\frac{g_p^2\omega}{4} + \frac{3\beta}{16\omega}\right)A_{\rm cr}^2. \qquad (10)$$

Based on this observation, we proceed with the simulations according to Eqs. (2)–(4) with the set of parameters given above. We choose $g_p = g_s = 1$ and start at $t = 0$ with a LM in the form of the first expression in Eq. (5) with a carrier wave number $q_p = 0.37$. For such a wave number the corresponding linear frequency is $\omega = 1.1856$. This frequency is located in the band gap of the spin wave spectrum and no localization transmission occurs in the case of small amplitudes, as it is seen from graph (a) of Fig. 3. According to relation (10) we can calculate the threshold amplitude for which localization transmission emerges and find $A_{\rm cr} = 0.22$. In the numerical results, transmission occurs for the incident LM amplitudes $A > 0.27$. This discrepancy can be explained by the fact that localization amplitudes in different parts of the multiferroic structure do not exactly coincide. In panel (b) of Fig. 3 we display the dynamics for a larger LM amplitude, i.e., $A = 0.33$, and find that localized excitations are formed in the ferromagnetic part as well. By further increasing the LM amplitude, the transmitted localization takes over almost all the energy of the incident one [graph (c) of the same figure]. If the amplitude of the incident LM is slightly below threshold (here $A = 0.265$), even a small perturbation may cause a transmission to the FM part. Thus, we add a term $\vec{f}(t)\vec{S}_1$ to the Hamiltonian (2) describing the action of a random magnetic field at the interface spins. $f(t)$ is uncorrelated in time and randomly distributed in the interval $[-f, f]$. For small random fields, $f = 0.05$, the picture is almost the same as for zero noise (cf. upper graphs of Figs. 3 and 4). Increasing the noise strength to a moderate

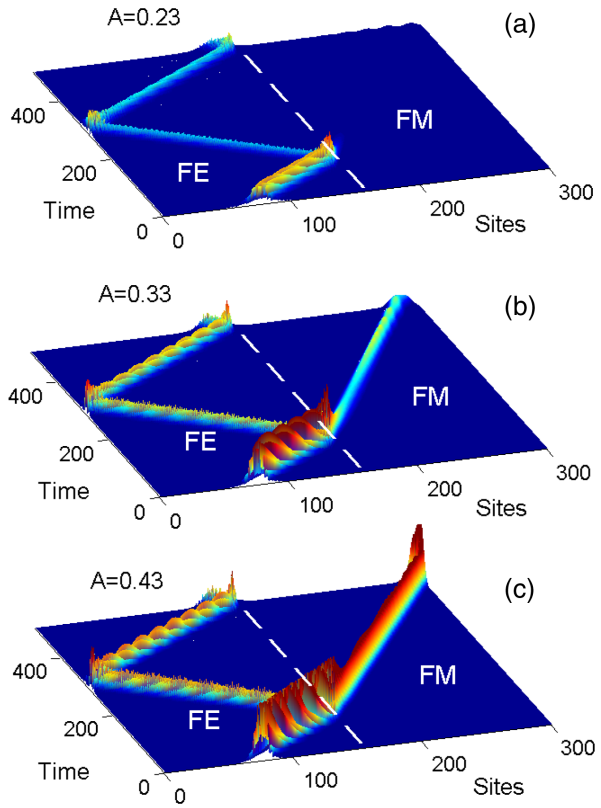

FIG. 3 (color online). This figure illustrates the dependence on the amplitude A of the LM reflection and transmission at the FE/FM interface. To this end we plot for different values of A the same quantity and choose the same parameters as in graphs (a)–(c) of Fig. 2 with $g_p = g_s = 1$. The scale is as in Fig. 2.

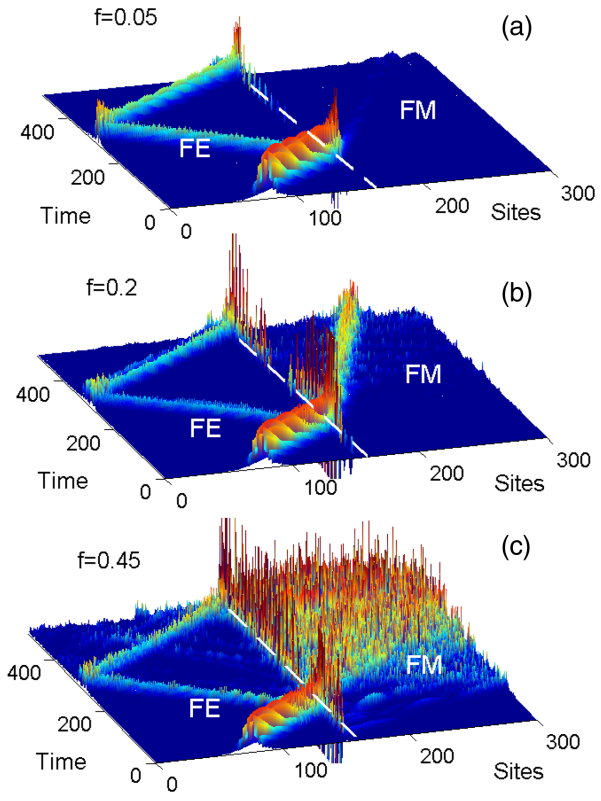

FIG. 4 (color online). Influence of noise on the LM reflection and transmission at the FE/FM interface illustrated by realizing similar simulations as in Fig. 3 but for $A = 0.265$ and including different noise levels as indicated on the graphs. Scale as in Fig. 2.

level, energy transmission in FM part takes place [see graph (b) of Fig. 4]. This stochastic resonancelike behavior is displayed in graph (c) of Fig. 4.

Summary.—As shown by analytical and numerical results, in a two-phase multiferroic the magnetoelectric coupling at the interface determines the conversion of an initial ferroelectric LM into a ferromagnetic signal, paving thus the way for FE and/or FM LM-based logic in multiferroics. As an essential step in this direction, we have identified the conditions under which a FE signal is converted into a FM one.

Consultations with Marin Alexe on the experimental realization are gratefully acknowledged. L. Ch., A. S., and J. B. are supported by DFG through Grant No. SFB 762 and No. SU 690/1-1. R. Kh. and S. R. are funded by a joint Grant from French CNRS and Georgian SRNSF (Grant No. 09/08), R. Kh. is supported by Grant No. 30/12 from SRNSF and S. R. acknowledge support of the contract LORIS (No. ANR-10-CEXC-010-01).

[1] W. Eerenstein, N. D. Mathur, and J. F. Scott, Nature (London) **442**, 759 (2006).
[2] Y. Tokura and S. Seki, Adv. Mater. **22**, 1554 (2010).
[3] C. A. F. Vaz, J. Hoffman, Ch. H. Ahn, and R. Ramesh, Adv. Mater. **22**, 2900 (2010).
[4] F. Zavaliche, T. Zhao, H. Zheng, F. Straub, M. P. Cruz, P.-L. Yang, D. Hao, and R. Ramesh, Nano Lett. **7**, 1586 (2007).
[5] H. L. Meyerheim, F. Klimenta, A. Ernst, K. Mohseni, S. Ostanin, M. Fechner, S. Parihar, I. V. Maznichenko, I. Mertig, and J. Kirschner, Phys. Rev. Lett. **106**, 087203 (2011).
[6] R. Ramesh and N. A. Spaldin, Nat. Mater. **6**, 21 (2007).
[7] I. E. Dzyaloshinkskii, Sov. Phys. JETP **10**, 628 (1960).
[8] M. Bibes and A. Barthélémy, Nat. Mater. **7**, 425 (2008).
[9] M. Gajek, M. Bibe, S. Fusil, K. Bouzehouane, J. Fontcuberta, A. Barthélémy, and A. Fert, Nat. Mater. **6**, 296 (2007).
[10] D. Pantel, S. Goetze, D. Hesse, and M. Alexe, Nat. Mater. **11**, 289 (2012).
[11] C.-W. Nan, M. I. Bichurin, S. Dong, D. Viehland, and G. Srinivasan, J. Appl. Phys. **103**, 031101 (2008).
[12] J. van den Boomgaard, A. M. J. G. van Run, and J. van Suchtelen, Ferroelectrics **10**, 295 (1976).
[13] N. Spaldin and M. Fiebig, Science **309**, 391 (2005).
[14] M. Fiebig, J. Phys. D **38**, R123 (2005).
[15] C.-G. Duan, S. S. Jaswal, and E. Y. Tsymbal, Phys. Rev. Lett. **97**, 047201 (2006).
[16] M. Fechner, I. V. Maznichenko, S. Ostanin, A. Ernst, J. Henk, and I. Mertig, Phys. Status Solidi B **247**, 1600 (2010).
[17] J.-W. Lee, N. Sai, T. Cai, Q. Niu, and A. A. Demkov, Phys. Rev. B **81**, 144425 (2010).
[18] A. M. Kosevich, B. A. Ivanov, and A. S. Kovalev, Phys. Rep. **194**, 117 (1990).
[19] R. P. Cowburn and M. E. Welland, Science **287**, 1466 (2000); Appl. Phys. Lett. **72**, 2041 (1998).
[20] P. Wadhwa and M. B. A. Jalil, Appl. Phys. Lett. **85**, 2367 (2004).
[21] S. M. Mohseni *et al.*, Science **339**, 1295 (2013).
[22] F. Kh. Abdullaev, A. A. Abdumalikov, and B. A. Umarov, Phys. Lett. A **171**, 125 (1992).
[23] B. I. Swanson, J. A. Brozik, S. P. Love, G. F. Strouse, A. P. Shreve, A. R. Bishop, W. Z. Wang, and M. I. Salkola, Phys. Rev. Lett. **82**, 3288 (1999).
[24] U. T. Schwarz, L. Q. English, and A. J. Sievers, Phys. Rev. Lett. **83**, 223 (1999).
[25] G. Kopidakis, S. Aubry, and G. P. Tsironis, Phys. Rev. Lett. **87**, 165501 (2001).
[26] S. Flach and K. Kladko, Physica **127D**, 61 (1999).
[27] A. K. Bandyopadhyay, P. C. Ray, and V. Gopalan, J. Phys. Condens. Matter **18**, 4093 (2006).
[28] P. Giri, K. Choudhary, A. Sengupta, A. K. Bandyopadhyay, and P. C. Ray, J. Appl. Phys. **109**, 054105 (2011).
[29] P. Giri, K. Choudhary, A. S. Gupta, A. K. Bandyopadhyay, and A. R. McGurn, Phys. Rev. B **84**, 155429 (2011).
[30] A. K. Bandyopadhyay, P. C. Ray, L. Vu-Quoc, and A. R. McGurn, Phys. Rev. B **81**, 064104 (2010).
[31] R. Benzi, A. Sutera, and A. Vulpiani, J. Phys. A: Math. Gen. **14**, L453 (1981).
[32] L. Gammaitoni, P. Hänggi, P. Jung, and F. Marchesoni, Rev. Mod. Phys. **70**, 223 (1998).
[33] M. Alexe and D. Hesse, Ferroelectrics **433**, 53 (2012).
[34] *Physics of Ferroelectrics*, edited by K. Rabe, Ch. H. Ahn, and J.-M. Triscone (Springer, Berlin 2007).
[35] J. M. D. Coey, *Magnetism and Magnetic Materials* (Cambridge University Press, Cambridge, 2010).
[36] T. Cai, S. Ju, J. Lee, N. Sai, A. A. Demkov, Q. Niu, Z. Li, J. Shi, and E. Wang, Phys. Rev. B **80**, 140415(R) (2009).
[37] N. Sedlmayr, V. K. Dugaev, and J. Berakdar, Phys. Rev. B **79**, 174422 (2009).
[38] A. Sukhov, C.-L. Jia, P. P. Horley, and J. Berakdar, J. Phys. Condens. Matter **22**, 352201 (2010); P. P. Horley, A. Sukhov, C. Jia, E. Martínez, and J. Berakdar, Phys. Rev. B **85**, 054401 (2012); Europhys. Lett. **99**, 17 004 (2012); Ferroelectrics **428**, 109 (2012); J. Appl. Phys. **113**, 013908 (2013).
[39] S. Chikazumi, *Physics of Ferromagnetism* (Oxford University, New York, 2002).
[40] M. Oikawa and N. Yajima, Prog. Theor. Phys. Suppl. **55**, 36 (1974).
[41] N. Giorgadze and R. Khomeriki, Phys. Status Solidi (b) **207**, 249 (1998).
[42] See Supplemental Material at http://link.aps.org/supplemental/10.1103/PhysRevLett.111.117202 for the graphical illustration and analytical derivation of weakly nonlinear localized modes, as well as detailed description of applied simplifications and system parameters.
[43] V. Garcia, M. Bibes, L. Bocher, S. Valencia, F. Kronast, A. Crassous, X. Moya, S. Enouz-Vedrenne, A. Gloter, D. Imhoff, C. Deranlot, N. D. Mathur, S. Fusil, K. Bouzehouane, and A. Barthélémy, Science **327**, 1106 (2010).